Algal Research 89 (2025) 104047

Contents lists available at ScienceDirect

Algal Research

journal homepage: www.elsevier.com/locate/algal

Internal ploidy and heritable chromosome fragmentation in *Parachlorella kessleri*

Kotaro Ishii [a,b,1], Madoka Asano [c,1], Yusuke Kazama [a,d], Tsuyoshi Takeshita [e], Kateřina Bišová [f], Vilém Zachleder [f,2], Atsushi Toyoda [g], Tomoko Abe [a], Shigeyuki Kawano [c,e,*]

[a] RIKEN Nishina Center for Accelerator-Based Science, 2-1 Hirosawa, Wako, Saitama 351-0198, Japan
[b] Department of Radiation Measurement and Dose Assessment, Institute for Radiological Science, National Institutes for Quantum Science and Technology, 4-9-1 Anagawa, Inage-ku, Chiba 263-8555, Japan
[c] Department of Integrated Biosciences, Graduate School of Frontier Sciences, The University of Tokyo, 5-1-5 Kashiwa-no-ha, Kashiwa, Chiba 277-8561, Japan
[d] Department of Bioscience and Biotechnology, Fukui Prefectural University, 4-1-1 Kenjojima, Matsuoka, Eiheiji-cho, Yoshida-gun, Fukui 910-1195, Japan
[e] Functional Biotechnology Project, Life Science Data Research Center, Graduate School of Frontier Sciences, 503 Kashiwanoha Campus Station Satellite, The University of Tokyo, 178-4-4 Wakashiba, Kashiwa, Chiba 277-0871, Japan
[f] Laboratory of Cell Cycles of Algae, Centre Algatech, Institute of Microbiology of the Czech Academy of Sciences, 37981 Třeboň, Czech Republic
[g] Department of Genomics and Evolutionary Biology, National Institute of Genetics, 1111 Yata, Mishima, Shizuoka 411-8540, Japan

ARTICLE INFO

Keywords:
Parachlorella kessleri
Heavy-ion beam
Internal ploidy
Mutation

ABSTRACT

Parachlorella kessleri is a unicellular green alga. Its ability to produce starch and neutral lipids makes it a valuable bioresource for biomass production. In green algae, the cell cycle with multiple fission shows different patterns in different species. Nevertheless, the basic understanding of the cell cycle and division in *P. kessleri* is still incomplete. Seven A chromosomes and three B chromosomes ($n = 7 + 3B$) were identified by microscopic observation and pulsed-field gel electrophoresis. The nuclear DNA content was then calculated. When the mean nuclear DNA content in the stationary phase was designated as 1C, the nuclear DNA content in the logarithmic growth phase ranged from 1.1C to 9.7C. In contrast, the chromosome number remained constant during the logarithmic growth phase, indicating that *P. kessleri* chromosomes underwent endoreduplication during multiple fission.

P. kessleri cells were irradiated with heavy-ion beams at 640, 290, and 30 keV/μm linear energy transfer (LET). Chromosome fragmentation was observed for each irradiation group. The number of chromosomes in the cells tended to increase with increasing LET and with increasing dose. Some fragmented chromosomes were observed to be stably inherited after repeated subculture. To facilitate mutation analysis, we refined the reference genome sequence of *P. kessleri*, resulting in 52 scaffolds with 2.5 Mbp of N50 and a 98.3 % BUSCO value. Genome-wide mutation analysis of the mutants with stable fragmented chromosomes revealed translocations. In the two mutants irradiated with 290 keV/μm LET, translocations affecting telomeric repeat sequences were detected, which may have contributed to the stability of the fragmented chromosomes. In addition, large-scale duplication and deletion were observed in the two mutants irradiated with 290 keV/μm LET. These findings indicated the potential utility of a heavy-ion beam as a mutagen for microalgae, inducing large-scale mutations in numerous genes leading to novel phenotypic mutants.

1. Introduction

Parachlorella kessleri is a unicellular green alga belonging to the order Chlorellales of the class Trebouxiophyceae. Depending on the culture conditions, *P. kessleri* can produce both starch and neutral lipids. This property makes it a valuable bioresource for biomass production, which

* Corresponding author at: Functional Biotechnology Project, Life Science Data Research Center, Graduate School of Frontier Sciences, 503 Kashiwanoha Campus Station Satellite, The University of Tokyo, 178-4-4 Wakashiba, Kashiwa, Chiba 277-8561, Japan.
E-mail addresses: ishii.kotaro@qst.go.jp (K. Ishii), ykaze@fpu.ac.jp (Y. Kazama), takeshita.tsuyoshi@edu.k.u-tokyo.ac.jp (T. Takeshita), bisova@alga.cz (K. Bišová), atoyoda@nig.ac.jp (A. Toyoda), tomoabe@riken.jp (T. Abe), kawano@edu.k.u-tokyo.ac.jp (S. Kawano).
[1] These authors equally contributed to this work.
[2] Deceased.

https://doi.org/10.1016/j.algal.2025.104047
Received 4 December 2024; Received in revised form 10 March 2025; Accepted 16 April 2025
Available online 17 April 2025

is of great interest in algal biotechnology [1–4]. Although extensive information is available on the production of starch and neutral lipid under different culture conditions, basic information on the cell cycle and division in *P. kessleri* is lacking.

In green algae, division into four or more daughter cells is common and is referred to as multiple fission, with the cell cycle following two main patterns, Scenedesmus and Chlamydomonas types [5–9]. In Scenedesmus-type cells, DNA replication and nuclear fission occur intermittently, according to the number of daughter cells formed, resulting in multinucleated cells. After the last nuclear division, protoplast fission occurs successively to form daughter cells. In contrast, Chlamydomonas-type cells remain mononuclear throughout their cell cycle, as nuclear division and protoplast fission alternate to form daughter cells, preventing multinucleation. Patterns combining these two major types have also been reported. For example, in *Haematococcus pluvialis*, DNA replication occurs once, followed by a series of nuclear and protoplast fissions, resulting in a multinucleated state [10]. In *P. kessleri*, DNA replication occurs once according to the number of daughter cells, followed by a continuous alternation of nuclear division and protoplast fission, with no multinucleate cells observed during the cell cycle [8,10]. As in the Chlamydomonas type, no multinucleated cells are formed during the cell cycle [5,8].

Internal ploidy in eukaryotes changes mainly through nuclear mitosis or nuclear duplication [11]. In normal cell division, DNA replication is followed by chromosome aggregation. The chromosomes align parallel to the equatorial plane of the cell and are distributed by the spindle to the two poles. This is followed by cytoplasmic division. In endomitosis, a rare phenomenon in plants, there is neither spindle formation nor loss of the nuclear membrane. Only replication and chromosome segregation take place, resulting in cells with an increased number of chromosomes [12]. In contrast, during endoreduplication, the main cause of increased internal ploidy in land plants (especially angiosperms), only DNA replication occurs, with sister chromatids remaining attached to each other and forming polytene chromosomes [12–14]. Microalgae typically have small nuclei, and there are few reports of karyotypic analyzes of species of the Trebouxiophyceae and related classes [15–18]. Currently, there are no reports of karyotyping in *P. kessleri*, so the number of chromosomes and the occurrence of endomitosis or endoreduplication after DNA replication are unclear.

Heavy-ion beams, a type of ionizing radiation, are often used for mutation breeding in plants due to their effectiveness as mutagens [19–25]. Heavy-ion beams have a higher linear energy transfer (LET) than X-rays or γ-rays, which allows them to induce localized, large-scale mutations [20,26,27]. The resulting mutants are considered more efficient because they have a lower risk of carrying deleterious mutations at the same time [20]. Heavy-ion beams have also been shown to be effective in improving the efficiency of biomass production in *P. kessleri* [28,29]. The *P. kessleri* mutant strain PK4, which was generated by irradiation with carbon-ion beams with an LET of 30 keV/μm, is one of the strains with the highest oil production under outdoor autotrophic mass culture conditions [28]. A comparison of mutations induced by heavy-ion beams with 30 keV/μm and 290 keV/μm LET in *Arabidopsis thaliana* revealed that a higher LET leads to more frequent chromosomal rearrangements [30]. It has been suggested that large-scale mutations can be efficiently induced by choosing the appropriate LET for the target species [31]. However, there are no reports on irradiation of *P. kessleri* with heavy-ion beams with higher LET, such as 290 keV/μm, so the potential to obtain mutants with unprecedented properties remains unexplored.

Genome sequence information is crucial for both basic and applied research, including mutation breeding. Ota et al. [32] reported a draft genome of *P. kessleri*. Genome sequencing was performed on strain PK4, and three genes responsible for high lipid productivity were identified by mapping the genome sequence and mutational analysis [29]. In addition, CRISPR/Cas9-mediated genome editing technology has shown that the *AATPL1* gene contributes to improved lipid productivity [33]. However, the draft genome of PK4 irradiated with a heavy-ion beam consists of 400 scaffolds with an average size of 156 kbp, making it difficult to detect large-scale mutations such as translocations. Recently, the development of large-scale sequencing technologies has made it possible to generate genome sequences at the chromosome or telomere-to-telomere (T2T) level for different species. Chromosome-level genome sequences have been obtained for microalgae species including *Chlamydomonas reinhardtii* [34], *Chromochloris zofingiensis* [35], *Pedinomonas minor* [36], and *Prymnesium parvum* [37]. Genome sequencing at the T2T level was performed on *Phaeodactylum tricornutum* [38].

In this study, we investigated the chromosome number of *P. kessleri* in metaphase and the behavior of DNA ploidy during multiple fission by microscopic examination of the cells. Exposure of *P. kessleri* to a high-LET heavy-ion beam resulted in a mutant with stable fragmented chromosomes. The draft genome sequence was refined using large-scale sequencing techniques. Mutational analysis using the refined genome sequence revealed complex chromosomal rearrangements in the mutant. This study provided important information for the development of algal biotechnology through mutation breeding.

2. Materials and methods

2.1. Strain and culture conditions

The cultures of *P. kessleri* (NIES-2152) were obtained from the Microbial Culture Collection of the National Institute for Environmental Studies (Tsukuba, Japan). Cells were cultured in 30 ml of TAP medium [32] under a 12:12 h light:dark cycle at 30 ± 10 μmol photons/m^2/s − 1 and 23 °C.

2.2. Karyotyping and DNA content determination

The cells of *P. kessleri* cells were cultured cultivated for 16–20 h under continuous light condition. A 1-ml sample of the culture was centrifuged at 3260*g* for 20 s and the supernatant was removed. The cells were then fixed in 0.75 % glutaraldehyde for at least 30 min at room temperature. After another centrifugation at 3260*g* for 20 s, the supernatant was removed and the cells were stained with SYBR Green I (Molecular Probes, Eugene, OR, USA) diluted 5000-fold in DMSO for 30 min. After centrifugation at 3260*g* for 20 s and removal of the supernatant, K buffer (10 mM Tris-HC1 buffer, pH 7.6, containing 0.25 M sucrose, 1 mM EDTA, 0.2 mM spermine, 0.4 mM spermidine, 0.25 % NaCl and 0.05 % 2-mercaptoethanol) [39] was added.

To quantify nuclear DNA content during interphase, fluorescent beads (SPHERO Fluorescent Nile Red Particles, Low Intensity, Spherotech, Libertyville, IL, USA) were mixed with 1/10 volume of the K buffer. To quantify the nuclear DNA content in which mitotic chromosomes appeared, the 160 kbp bacteriophage T2 [40] (ATCC, VA, USA) was used instead of fluorescent beads. Bacteriophage T2 was prepared according to the manufacturer's instructions and diluted with K buffer. Microscopic images were taken with an upright microscope DM6000B (Leica, Germany) and a monochrome digital CCD camera DFC360 FX (Leica, Germany). ImageJ v 1.47 [41] and LAS AF Lite (Leica, Germany) were used to measure fluorescence intensity.

The nuclear DNA content during interphase was calculated by measuring the relative fluorescence intensity of the nuclei in relation to that of the fluorescent beads. The nuclear DNA content during the mitotic phase, on the other hand, was calculated by measuring the relative fluorescence intensity of the individual chromosomes in relation to that of bacteriophage T2 and then summing the values. In the absence of bacteriophage T2 near the chromosomes, the relative SYBR Green I fluorescence intensity of the chloroplast nucleoids was used as a reference.

Chloroplasts typically have ~100 copies of the genome, and multimeric chloroplast DNA (cpDNA) molecules are organized into cpDNA-RNA-protein complexes (i.e., chloroplast nucleoids). The amount of

chloroplast nucleoid DNA varies during the lifecycle of algae [42]. The relative fluorescence intensity of chloroplast nucleoids seen above the red autofluorescence of *P. kessleri* chloroplasts in logarithmic growth and stationary phase, was measured with respect to the fluorescence intensity of the 160 kbp T2 phage (Supplementary Fig. 1a). The calculated DNA content of the chloroplast nucleoids in the logarithmic growth phase was 1.4 Mbp for the mode and 2.5 Mbp for the mean (Supplementary Fig. 1b). The mean value in the stationary phase was 340 kbp (Supplementary Fig. 1c). The DNA content of each chromosome was calculated by measuring the relative fluorescence intensity with respect to that of the chloroplast nucleoid. The DNA content during the mitotic phase was determined by summing the DNA content of all chromosomes.

2.3. Pulsed-field gel electrophoresis (PFGE)

P. kessleri cells were cultured in 30 ml TAP medium under a 16:8 h light:dark cycle until the total cell number reached at least 3×10^8 cells. After centrifugation at 3260*g* for 20 s, the medium was replaced with fresh TAP medium, and the cells were cultured for another day. The cells were then washed with 0.05 M EDTA (pH 8.0), centrifuged again and the supernatant was removed. The remaining cells were suspended in a 1:1 mixture of 0.05 M EDTA and 2 % CleanCut Agarose (Bio-Rad Laboratories, Hercules, CA, USA) in a volume of 50 μL per 1.5×10^8 cells. Plugs were prepared by placing the cell suspension into the wells of a disposable plug mold (Bio-Rad Laboratories) and left overnight at 4 °C. Plugs were incubated overnight at 37 °C in LET buffer (10 mM Tris-HCl pH 7.5, 0.45 M EDTA pH 8.0, 7.5 % 2-mercaptoethanol), washed three times with 0.5 M EDTA, and then incubated in NDS buffer (10 mM Tris-HCl pH 7.5, 0.445 M EDTA pH 8.0, 1 % SDS, 1 mg/ml proteinase K) for 4 h at 50 °C. PFGE was performed using the CHEF Mapper XA (Bio-Rad Laboratories) under two conditions: (i) a voltage gradient of 2.3 V/cm with a linear switching time of 600 to 1800 s for 72 h and a reorientation angle of 106° and (ii) a voltage gradient of 2 V/cm with a constant switching time of 30 min for 72 h and a reorientation angle of 106°. The buffer was circulated, cooled to 14 °C and changed every 24 h during PFGE. Gels were stained with GelRed Nucleic Acid Gel Stain (Wako, Japan) for 30 min and photographed using the ChemiDoc XRS+ system with Image Lab Software (Bio-Rad Laboratories).

2.4. Refining the genome sequence

Genomic DNA of *P. kessleri* (NIES-2152) was isolated using QIAGEN Genomic-tips (Qiagen, Hilden, Germany) and sheared into fragments of 20–50 kbp using a g-tube device (Covaris Inc., Woburn, MA, USA). An SMRTbell library was prepared using a Template Prep Kit v 1.0 (Pacific Bioscience, Menlo Park, CA, USA) according to the manufacturer's protocol. The sequencing library was size-selected using the BluePippin system (Sage Science, Beverly, MA, USA) with a minimum fragment length cutoff of 17 kbp and sequenced on the PacBio RSII sequencer with SMRT cell v 3 and P6-C4 v 2 chemistry, yielding 835,735 subreads (11.8 Gbp). PacBio reads were assembled using the program canu assembler (v 2.1.1) [43] with the parameter "genomeSize = 69 m". The assembled contigs were error-corrected using Arrow (v 9, in SMRT Link) with the default settings. For further error correction, 8.82 Gbp of 2 × 250 bp paired-end sequencing generated with the HiSeq 2500 sequencing system (Illumina, San Diego, CA, USA) was used to improve the base quality of the assembled sequence using the software tool Pilon (v 1.23) [44] with the parameter "–fix indel". Scaffolding was performed using the software LRScaf (v 1.1.12) [45] with default settings. Contamination checks were performed using the software blastn (v 2.10.0) [46] with the parameter "-evalue 1e-10". Contig sequences were removed if hits to known organelle or bacterial genome sequences (RefSeq) covered >10 % of the total contig length. Contigs were also removed if their GC content was <2 % or >98 %. In addition, HiSeq reads were mapped to genome assemblies, achieving an average coverage of 137×. Contigs that had an average short short-read sequence coverage of <10× were considered to originate from contaminated genomes and were removed. Protein-encoding regions were predicted using the GeneMark-ES [47]. The Completeness of genomes was assessed using BUSCO [48].

2.5. Identification of putative chromosome ends and centromeres

To identify chromosome ends, a homology search was performed for regions located 500 bp from the scaffold terminus of the genome sequence (v2) and in which the telomere repeat unit of Trebouxiophyceae (TTTAGGG) [49] was repeated more than five times in tandem. In addition, 5.10 Gbp of the 2 × 150 bp paired-end sequencing of *P. kessleri* genomic DNA (NIES-2152) generated with the HiSeq X ten sequencing system (Illumina) was mapped to the genome sequence (v2) using BWA-MEM (v 0.7.15) [50]. The mapping status of regions within 500 bp of the scaffold terminus was visually confirmed using IGV software [51]. Scaffold termini where telomeric repeats were identified by homology search or short-read mapping were labeled as putative chromosome ends.

Potential centromeres were identified as regions with low GC content, as was already the case with *Cyanidioschyzon merolae* [52]. The genome sequence was divided into 3-kbp segments and the GC content for each segment was determined. Regions in which 3-kbp segments with a GC content of <55 % continued with breaks for >24 kb were assumed to be putative centromeres.

2.6. Heavy-ion beam-irradiated cell line establishment

P. kessleri cells in the late logarithmic growth phase were harvested and stored at 4 °C until irradiated with a heavy-ion beam. The cells were irradiated with carbon ions (30 keV/μm, 25–200 Gy), argon ions (290 keV/μm, 25–200 Gy) or iron ions (640 keV/μm, 25–200 Gy) in the RIKEN RI beam factory as previously described [26]. To induce mitosis, the cells were transferred to new TAP medium immediately after irradiation and incubated at 23 °C for 16–20 h under continuous light conditions. The cells were cultured on 1.5 % TAP agar medium for about 2 weeks and single colonies were isolated. The isolated cell lines were cultured in 30 ml TAP medium. After 1 week of cultivation, a subculture was performed by transferring 300 μl of the culture into a new 30 ml aliquot of TAP medium.

2.7. Whole-genome mutation analysis

DNA from *P. kessleri* cell lines was extracted as previously described [29]. Genome resequencing on Ar100–1-7C (generated by irradiation with 100 Gy argon-ion beam), C100–1-8H (100 Gy carbon-ion beam), Fe200–1-1H (200 Gy iron-ion beam), Shino-9 (25 Gy carbon-ion beam), and Shino-7 (25 Gy carbon-ion beam) lines using a HiSeq 2500 sequencing system generated 4.3, 4.2, 4.4, 4.6 and 4.4 Gbp, respectively. 4.4 Gbp of 2 × 500 bp paired-end sequences, respectively. Genome resequencing of the Fe75–1-3H and Ar75–1-2C lines with a HiSeq X ten sequencing system generated 2.6 and 2.6 Gbp of 2 × 150 bp paired-end sequences, respectively. Mutational analysis was performed using the AMAP pipeline [53] as previously described [29]. Mutation candidates were visually confirmed using IGV software.

Annotation of genes that have lost function or are duplicated in the five cell lines Ar100–1-7C, Fe200–1-1H, Fe75–1-3H, and Ar75–1-2C was performed with the BLASTX program (e-value cut-off of 1E-4), using the NCBI-RefSeq database (plant). The presence of homologous genes in the genome was investigated with the TBLASTX program (e-value cut-off of 1E-4) using the gene set of the genome as database. In addition, the sequences of 811 essential genes in *A. thaliana* [31] were used as a database to investigate homology using the BLASTX program (e-value cut-off of 1E-4).

3. Results

3.1. Karyotype analysis of P. kessleri

To observe the metaphase chromosomes of *P. kessleri*, the cells were stained with SYBR Green I during the logarithmic growth phase to visualize the chromosomes (Fig. 1a, b). As a rule, ten chromosomes were observed on each image. Chromosome counting in 80 cells revealed a range of 5–11 chromosomes, with seven being the most abundant (Fig. 2a). Chromosomal DNA was extracted and separated by PFGE, resulting in bands of 4.1 Mbp, 2.3 Mbp, 1.6 Mbp, 0.9 Mbp and 0.2 Mbp (Fig. 1c). Chromosomes larger than 4.1 Mbp were indistinguishable. The intensity of the 4.1 Mbp band was approximately 1.8 times higher than that of the 2.3 Mbp band, consistent with the molecular weight ratio. However, the brightness of the 1.6 Mbp band was 5.4 times lower than that of the 2.3 Mbp band, which did not correspond to 1.4 times the molecular weight ratio. Based on this brightness ratio and the microscopic observations, it was estimated that only 20–27 % of cells contain chromosomes corresponding to 1.6 Mbp. B chromosomes may be present or absent within individuals of the same species population, and their number may vary [54]. Based on the frequency of its occurrence, this chromosome is considered a B chromosome and was designated as B1. Similarly, the brightness of the 0.9 Mbp band was 3.4 times less than that of the 2.3 Mbp band, which did not correspond to the molecular weight ratio of 2.6 times. Therefore, the corresponding chromosome was designated B2. In addition, the brightness of the 0.2 Mbp band was 6.1 times lower than that of the 2.3 Mbp band, which also did not correspond to the molecular weight ratio of 11.5 times. Therefore, the corresponding chromosome was designated B3. While only 76 % of the cells contained the B2 chromosome, the B3 chromosome was present with an average of 1.9 chromosomes per cell. *P. kessleri* therefore has seven A chromosomes and three B chromosomes, which are labeled A1–A7 and B1–B3 respectively.

3.2. Nuclear DNA content of P. kessleri

The nuclear DNA content during interphase was measured by staining the nuclei with SYBR Green I both in the logarithmic growth phase and in the stationary phase under continuous light conditions. The relative fluorescence intensity was measured together with fluorescent beads. The mean relative fluorescence intensity of the nuclei in the stationary phase was designated as 1C of the nuclear DNA content (Fig. 2b). In the logarithmic growth phase, the nuclear DNA content ranged from 1.1C to 9.7C, with an average of 4.3C (Fig. 2c).

The nuclear DNA content during mitosis was calculated by adding the DNA content of the individual chromosomes. The chromosomal DNA content was measured by the relative fluorescence intensity of T2 phage and chloroplast nucleoids. The nuclear DNA content ranged from 1C to 8C (Supplementary Fig. 2). Typical chromosome images are shown in Fig. 3. The nuclear DNA content is 2.1C (Fig. 3a), 4.5C (Fig. 3b), and 8.0C (Fig. 3c). However, the seven A chromosomes and three B chromosomes are observed in all cells, indicating that ploidy remained constant. This suggested that the chromosomes in *P. kessleri*, became polytene during multiple fission and endoreduplication occurred.

3.3. Chromosome fragmentation by heavy-ion beam irradiation

To investigate the mutations induced in *P. kessleri* by irradiation with

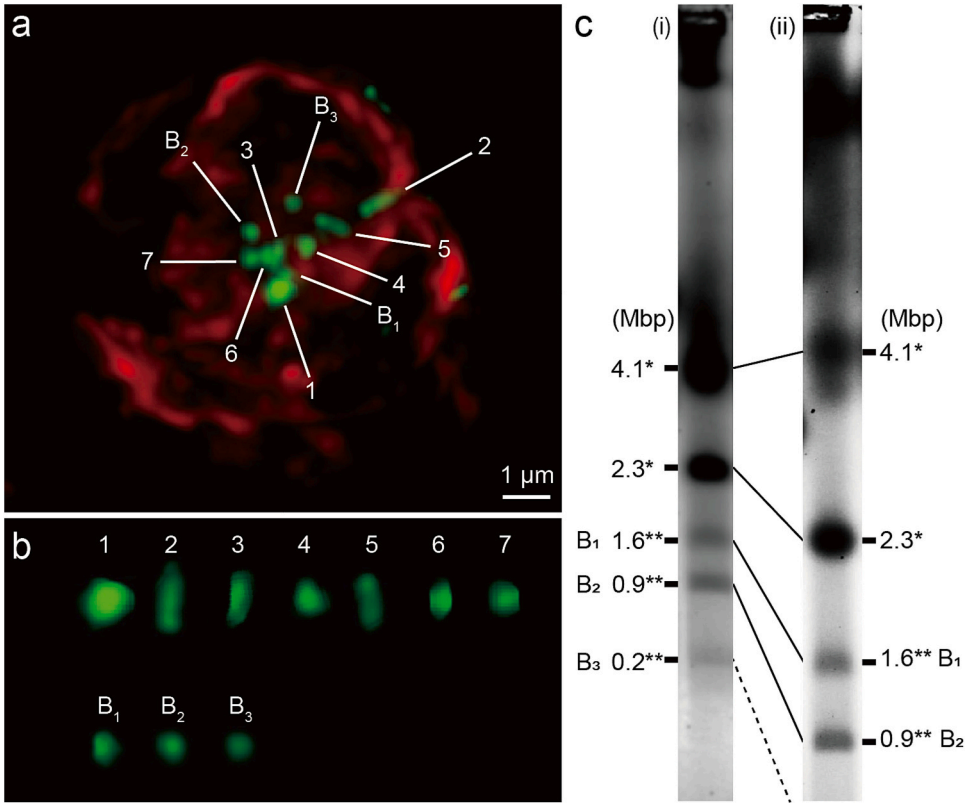

Fig. 1. Karyotype analysis of *P. kessleri*. (a) SYBR Green I stained image of a typical cell in the logarithmic growth phase. The position of the nucleus after SYBR Green I staining is shown in green. The autofluorescence of the chloroplasts is shown in red. Bar = 1 μm. (b) Karyogram of the typical cell. The numbers above the chromosomes indicate the chromosome number. B1–B3 indicate the chromosome number of the B chromosome. (c) PFGE patterns of chromosomes extracted from cells in the logarithmic growth phase. The respective electrophoretic conditions are described in Materials and methods. Under condition (ii), the 0.2 Mbp band flows out of the gel, but the resolution of the other bands is improved. The numbers indicating the band sizes are marked with one or two asterisks to distinguish between A and B chromosomes. (For interpretation of the references to colour in this figure legend, the reader is referred to the web version of this article.)

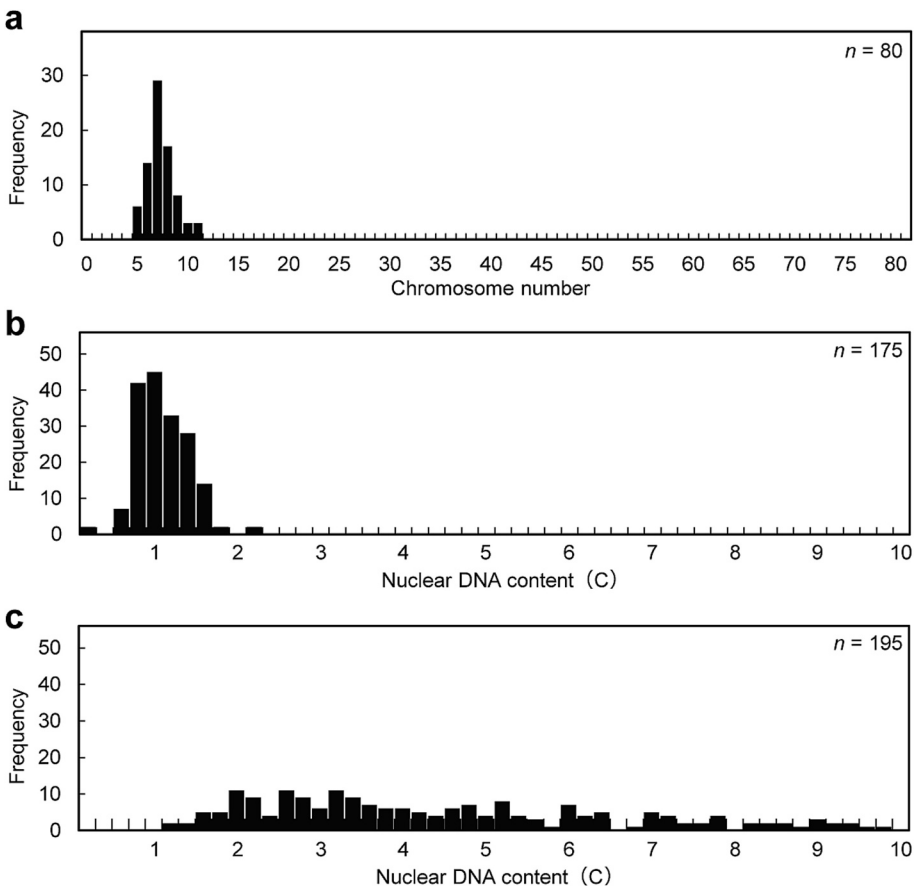

Fig. 2. Number of chromosomes of cells in the logarithmic growth phase (a) and distribution of the nuclear DNA content in the cells in the stationary (b) and logarithmic growth phase (c). The mean relative fluorescence intensities of the cell nuclei in the stationary phase were designated as 1C.

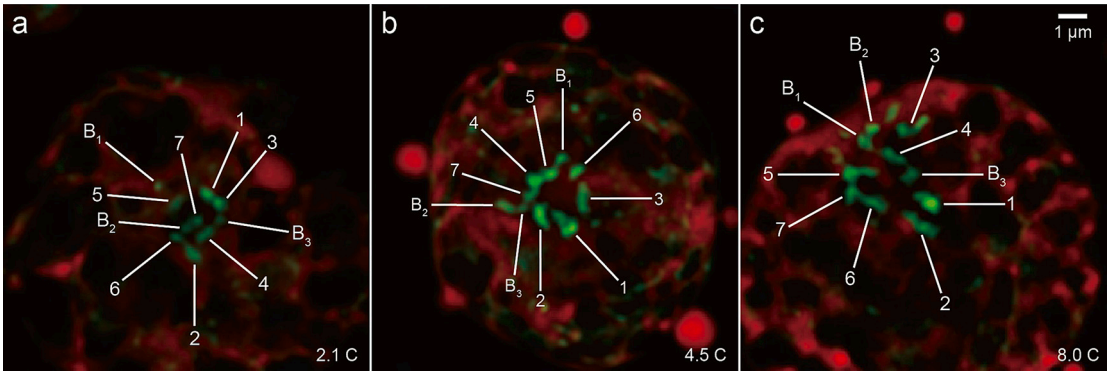

Fig. 3. Typical mitotic nuclei with emerging chromosomes during the logarithmic growth phase. The seven A chromosomes and three B chromosomes stained with SYBR Green I are shown in green. Chlorophyll autofluorescence of the chloroplasts is shown in red, and the chloroplast nucleoids are shown in green, which appears to overlay the autofluorescence. The relative fluorescence intensity of T2 phage or chloroplast nucleoids was used to calculate the DNA content of each chromosome. The DNA content during the mitotic phase was determined by summing the DNA content of all chromosomes. The nuclear DNA contents were calculated as 2.1C (a), 4.5C (b) and 8.0C (c), respectively. Bar = 1 μm. (For interpretation of the references to colour in this figure legend, the reader is referred to the web version of this article.)

heavy-ion beams at relatively high LET, the cells were exposed to iron-ion beams with 640 keV/μm LET, argon-ion beams with 290 keV/μm LET, and carbon-ion beams with 30 keV/μm LET in the range of 0–75 Gy during the logarithmic growth phase. The cells were cultivated under continuous light and the chromosomes were stained with SYBR Green I. Cells with fragmented chromosomes were observed (Fig. 4a). The calculated nuclear DNA contents, measured as relative fluorescence intensities on typical chromosome images, ranged from 1.8C to 4.5C (Fig. 4b–j, Supplementary Table 1), falling within the distribution of nuclear DNA content during logarithmic growth of non-irradiated cells. This indicated that the increased chromosome number is due to DNA double-strand breaks caused by irradiation with heavy-ion beams and not due to nuclear fission.

In each irradiation group, the number of chromosomes in the cells tended to increase with increasing LET and dose (Fig. 2a, Fig. 5a–f, Fig. 6a, b, e). In particular, 14 % of the cells exposed to 75 Gy iron-ion beam had >30 fragmented chromosomes (Fig. 6e). To determine the stability of the fragmented chromosomes, cell populations exposed to

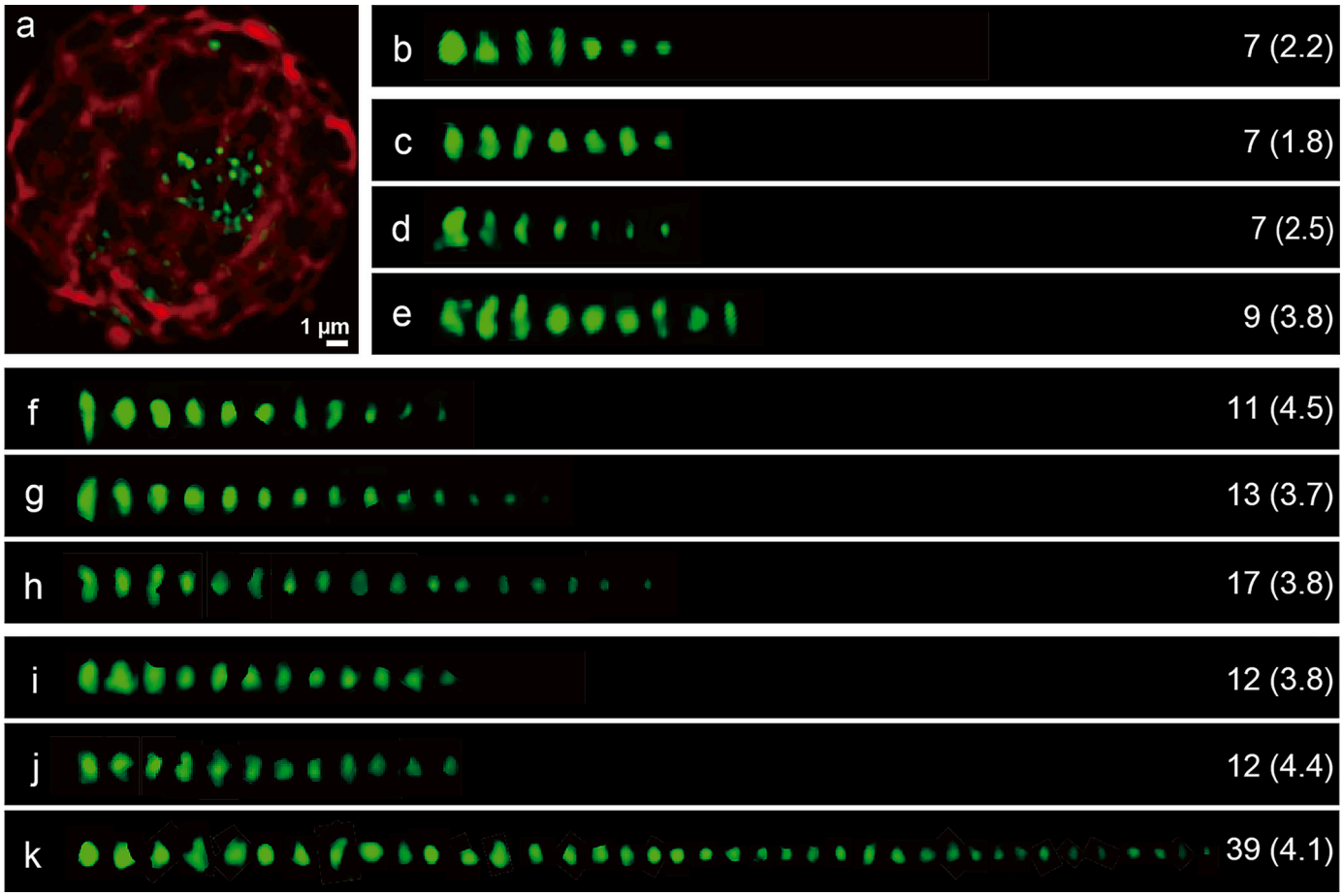

Fig. 4. Karyotype analysis of cells after heavy-ion beam irradiation. (a) SYBR Green I stained image of a typical unirradiated cell in the logarithmic growth phase. The position of the cell nucleus is shown in green. The autofluorescence of the chloroplasts is shown in red. Bar = 1 μm. (b–k) Karyogram of a typical cell after irradiation in each group. The chromosome number and nuclear DNA amount (C) in parentheses of each cell is shown in the right corner after irradiation with: (b) unirradiated control, (c-e) carbon-ion beams at 25 Gy (c), 50 Gy (d), and 75 Gy (e), (f-h) argon-ion beams at 25 Gy (f), 50 Gy (g), and 75 Gy (h), (i-k) iron-ion beams at 25 Gy (i), 50 Gy (j), and 75 Gy (k). (For interpretation of the references to colour in this figure legend, the reader is referred to the web version of this article.)

50 Gy and 75 Gy iron-ion beam were subcultured. The number of chromosomes tended to decrease with repeated subcultures (Fig. 6c, d, f, g). Thus, irradiation with heavy-ion beams caused chromosome fragmentation, but unstable chromosome fragments without centromeres or telomeres could not be preserved and dropped out during subculture. However, after four subcultures, 9.7 % of the cells irradiated with 50 Gy iron-ion beams and 3 % of the cells irradiated with 75 Gy still had >20 chromosomes (Fig. 6d, g), which indicates that fragmented chromosomes persist even after cell division.

3.4. Reference genome sequence refinement

The chromosome fragmentation could be due to chromosome rearrangement as a result of irradiation with heavy-ion beam beams. The genome sequence of *P. kessleri* reported so far is a draft genome sequence (v1) with an average length of 156 kbp [32], which is not suitable for large-scale mutation analyzes such as chromosomal rearrangements. To improve the reference genome sequence for such analyzes, genomic DNA of *P. kessleri* strain NIES-2152 was extracted and sequenced with PacBio RSII/Sequel to obtain long-read sequences. The long-read sequence was assembled and calibrated with the short-read sequence used to generate the draft genome. The result was a 62.7 Mbp genome sequence (v2) consisting of 52 scaffolds (Supplementary Table 2). Analysis of the completeness of the genome showed an increase from 95.8 % Chlorophyta orthologs in the original genome sequence (v1) to 98.3 % in the refined genome sequence (v2).

Chromosome ends were identified by a homology search of the telomere sequence of Trebouxiophyceae (TTTAGGG) and mapping of short-read sequences containing telomeric repeats on the genome sequence. Telomeric repeats were assigned to 26 scaffold end regions, which were designated as putative chromosome ends (Supplementary Fig. 3).

Potential centromeres in *P. kessleri* were identified by splitting the genome sequence into 3-kbp segments and determining the GC content for each segment. Eight regions with low GC content, excluding terminal regions, were identified as putative centromeres (Supplementary Fig. 3). Scaffold_9 (3.9 Mb) had telomeric repeat sequences at both ends and an internal putative centromere, indicating a chromosome sequence at the T2T level.

3.5. Mutants with stable fragmented chromosomes

To further investigate chromosome fragmentation, *P. kessleri* was irradiated with carbon-, argon-, and iron-ion beams at 100–200 Gy. The cells from each irradiation group, including those exposed to 75 Gy argon and 75 Gy iron-ion beams, were cultured on agar medium to isolate single colonies and establish cell lines. The nuclear DNA of seven lines was analyzed by PFGE. Four lines, Fe75–1-3H (produced by irradiation with 75 Gy iron-ion beams), Ar75–1-2C (75 Gy argon-ion beams), Ar100–1-7C, and C100–1-8H, showed banding patterns that differed from the wild type (Fig. 7). The Fe75–1-3H line lost a band on chromosome 7 (2.3 Mbp), Ar75–1-2C lost a band on chromosome 7 and

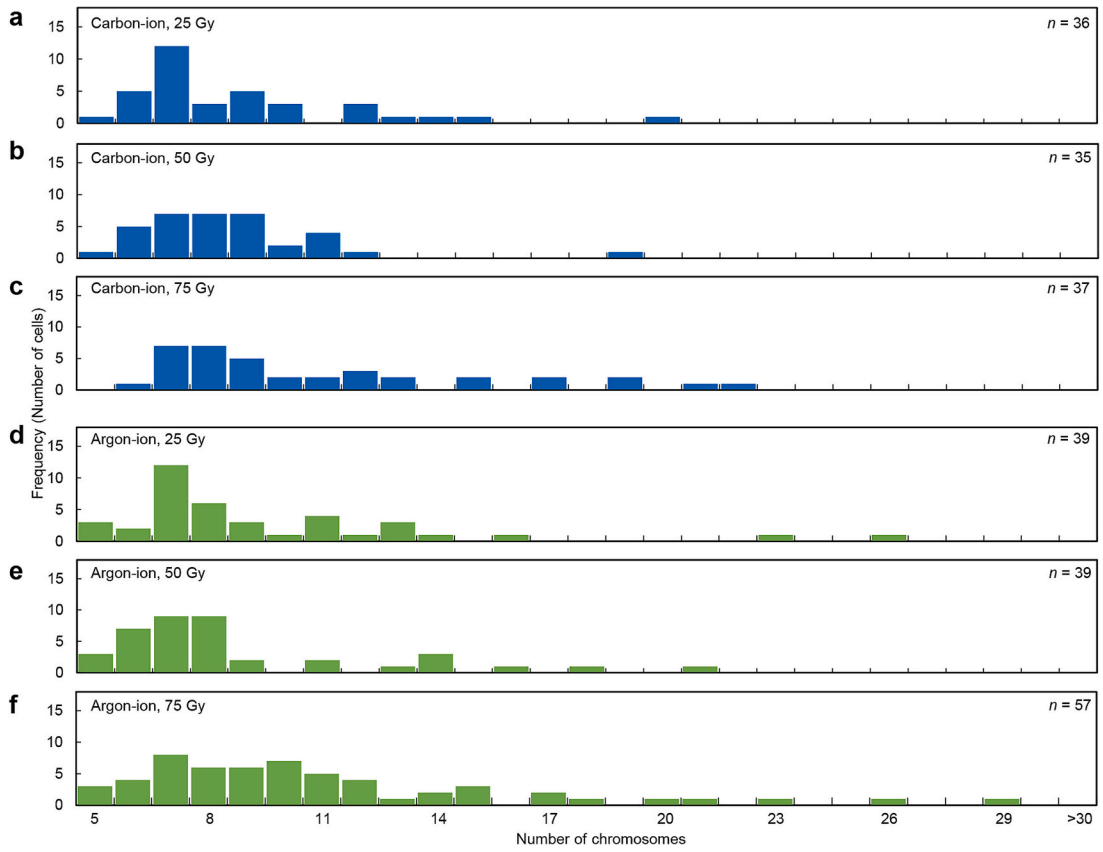

Fig. 5. Chromosomal distribution in cells after irradiation with: (a-c) carbon-ion beams at 25 Gy (a), 50 Gy (b), 75 Gy (c), (d-f) argon-ion beams at 25 Gy (d), 50 Gy (e), and 75 Gy (f).

gained new bands of approximately 1.9 Mbp and 0.6 Mbp, Ar100–1-7C lost a band on chromosome B2 (0.9 Mbp) and gained a new band of 1.3 Mbp, and C100–1-8H gained new bands of 1.4 Mbp and 1.3 Mbp. The chromosomes corresponding to the lost bands may have fragmented and been lost during subculture or combined with larger chromosomes by translocation.

Genome resequencing was performed on five lines (Fe75–1-3H, Fe200–1-1H, Ar75–1-2C, Ar100–1-7C and C100–1-8H) and two lines (Shino-9 and Shino-7) generated by irradiation with 25 Gy carbon-ion beams. A mutation analysis focusing on chromosomal rearrangements was carried out. Junctions corresponding to large-scale mutations of >100 bp were detected in a Shino-9 line and not in the Shino-7 line. In contrast, the Ar75–1-2C, Ar100–1-7C, Fe75–1-3H and Fe200–1-1H lines had 12, 17, 10 and 29 (including one insertion) junctions, respectively (Fig. 8, Supplementary Tables 3 and 4). All junctions except those detected in duplicated regions or at their borders were homozygous. Junctions with telomeric repeat regions were detected in lines Ar75–1-2C and Ar100–1-7C, possibly indicating new terminal segments of fragmented chromosomes. In addition, line Ar75–1-2C showed a 157-kbp duplication of genomic regions (Scaffolds_16 and part of Scaffolds_47 linked by translocation) (Supplementary Table 4). The Ar100–1-7C line had a 207-kbp deletion in Scaffolds_5 (Supplementary Table 4).

We analyzed the mutated putative genes in five cell lines in which chromosomal rearrangements were detected. Breakpoints at 134 sites resulted in translocations or deletions, leading to loss of function of 61 genes (Table 1, Supplementary Table 5). Of these, 38 genes showed similarity to known genes, and 8 genes were similar to essential genes in *A. thaliana*. However, the five cell lines did not show any conspicuous phenotypic abnormalities. This could be due to the presence of genes with multiple copies. Upon examination, it was found that most of the 38 genes were multicopy genes and with only 3 were considered single-copy genes.

4. Discussion

4.1. Chromosome dynamics of *P. kessleri*

P. kessleri is a species of algae of biotechnological importance due to its ability to overproduce starch and neutral lipids under certain growth conditions [1,4]. The production of these compounds can be induced by inhibiting cell division during the cell cycle [1,4]. Understanding the basic biology of *P. kessleri* is essential for further industrial applications. In a previous study, Zachleder et al. [9] developed a method for synchronous culture and showed that the cells remain mononuclear throughout the cell cycle while undergoing multiple fission. However, the state of the polyploid DNA after replication remained unclear. This study provided the first microscopic observations of endoreduplication during multiple fission in *P. kessleri* and revealed polytene chromosomes during nuclear fission, as indicated by an increase in nuclear DNA content to 8C, while chromosome number remained constant (Fig. 3).

B chromosomes or excess chromosomes usually have minimal genetic effects [55], which is why they are absent in some cell populations [56]. In this study, PFGE results showed that approximately 20 % of *P. kessleri* cells had three short chromosomes, indicating the presence of B chromosomes. Microscopic analysis frequently showed seven chromosomes, indicating that *P. kessleri* has a karyotype of $n = 7 + 3B$. B chromosomes are generally smaller than A chromosomes [57], with no known species having a B chromosome larger than its largest A chromosome [58]. The largest B chromosome in *P. kessleri* was estimated to be 1.6 Mb, smaller than the smallest A chromosome (chromosome 7) at 2.3 Mb, which is consistent with the typical characteristics of B

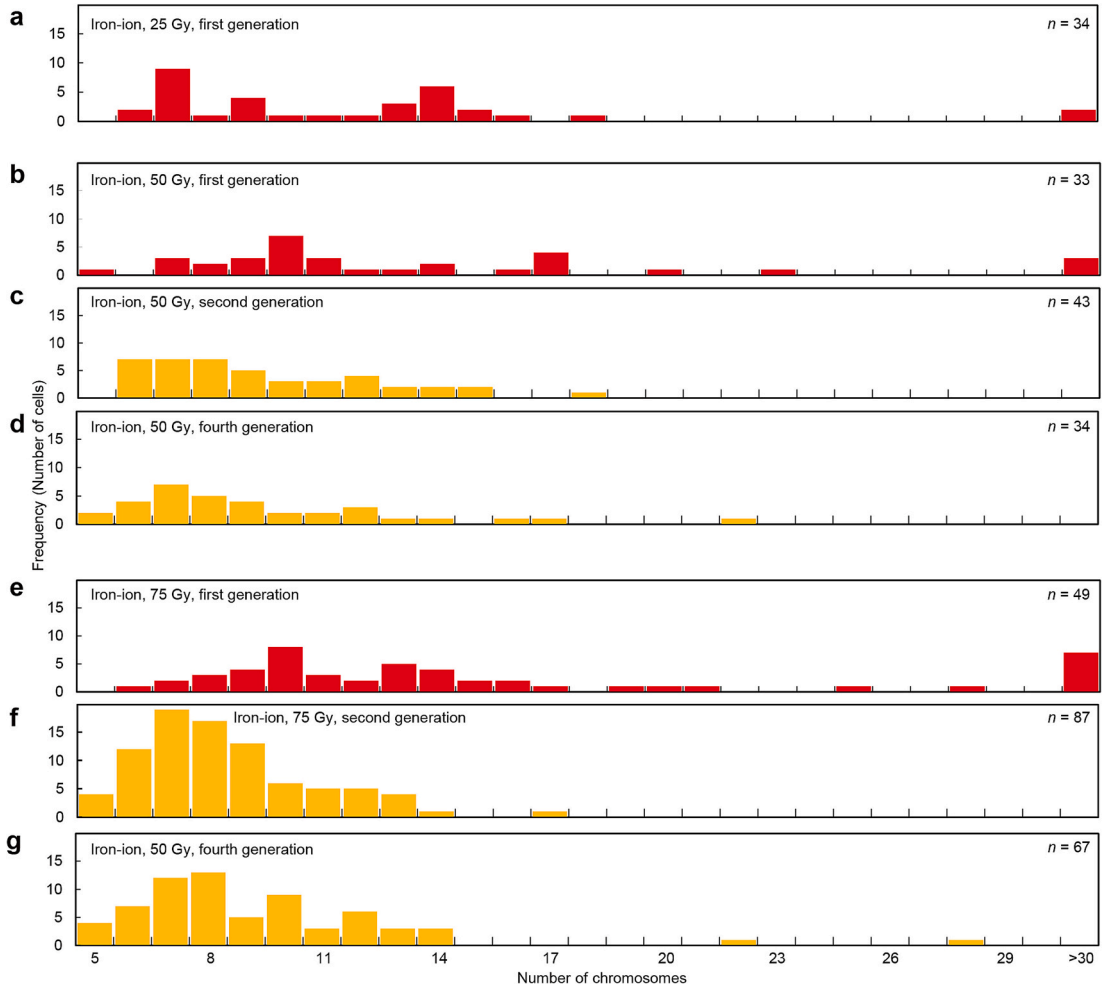

Fig. 6. Effects of subculture on chromosome distribution after iron-ion beam irradiation. (a) First generation after 25 Gy irradiation. (b) First generation after 50 Gy irradiation. (c) Second generation after 50 Gy irradiation. (d) Fourth generation after 50 Gy irradiation. (e) First generation after 75 Gy irradiation. (f) Second generation after 75 Gy irradiation. (g) Fourth generation after irradiation of 75 Gy.

chromosomes.

In the class Trebouxiophyceae, chromosome numbers have been reported to range from 5 to 20 in species such as *C. variabilis* [59], *C. vulgaris* [60], *C. ellipsoidea* [60], *Coccomyxa subellipsoidea* [61], *Nannochloris bacillaris* [62], *Choricystis minor* [18], and *Choricystis chodatii* [18]. These determinations were based on karyotypic analysis through PFGE or microscopy, without reference to B chromosomes. Systematic information on B chromosomes in Trebouxiophyceae can be achieved through similar PFGE and microscopic analyses.

4.2. Toward obtaining T2T-level genome sequence

Microalgae species with a genome size of ≤20 Mbp, such as *Cyanidioschyzon merolae* [63], *Micromonas commoda* [64], and *Ostreococcus lucimarinus* [65], were sequenced using DNA cloning technology. Recent advancements in long-read sequencing technologies by Pacific Biosciences (PacBio) and Oxford Nanopore Technologies (ONT) have facilitated the sequencing of larger genomes. In *Chlorella* sp. SLA-04, a T2T genome sequence of 38.8 Mbp was achieved using ONT [66], and *Chlamydomonas reinhardtii* achieved a T2T genome of 114 Mbp using a combination of PacBio and ONT, despite missing some telomere sequences at three chromosome ends [34]. *Pedinomonas minor*'s genome was analyzed using short reads (Illumina HiSeq), long reads (PacBio), and Hi-C sequencing, yielding a 55.0 Mbp genome at the pseudochromosome level, but not at the T2T level [36]. Similarly, a genome sequence of 58 Mbp in 19 chromosomes was obtained for *Chromochloris zofingiensis* using Illumina, PacBio, and whole- genome optical mapping, but only 25 of the 38 chromosome ends were sequenced at the T2T level [35].

In this study, the genome of *P. kessleri* was refined by PacBio sequencing, reducing the number of scaffolds from 400 in the draft genome sequence to 52, resulting in a total length of 62.7 Mbp (Supplementary Table 2). BUSCO analysis revealed 98.3 % Chlorophyta orthologs in the refined genome, compared to 93.4 % in the T2T genome of *Chlorella* sp. SLA-04 [66]. This indicates that the refined genome sequence covers most of the genome of *P. kessleri*. The unsequenced gaps probably contain repeats that are difficult to sequence. The refined genome can be used as a reference for the detection of large-scale mutations; however, detailed information would require a combination of sequencing technologies.

Mapping the reads with telomeric sequences revealed 26 scaffold ends with telomeric repeats (Supplementary Fig. 1). Given the chromosome number of *P. kessleri* ($n = 7 + 3B$), it was assumed that some of these scaffold ends were chromosome ends, while others may have been internal telomeric repeats. GC content analysis identified eight A + T-rich regions, ranging from 23 to 79 kbp, as putative centromeres. However, based on chromosome number, two additional centromeres should exist. Immunological experiments with CENP-A antibodies, as used by Matsuzaki et al. (2004) [52] for *Cyanidioschyzon merolae*, were unsuccessful in the present study. Further experiments are required to

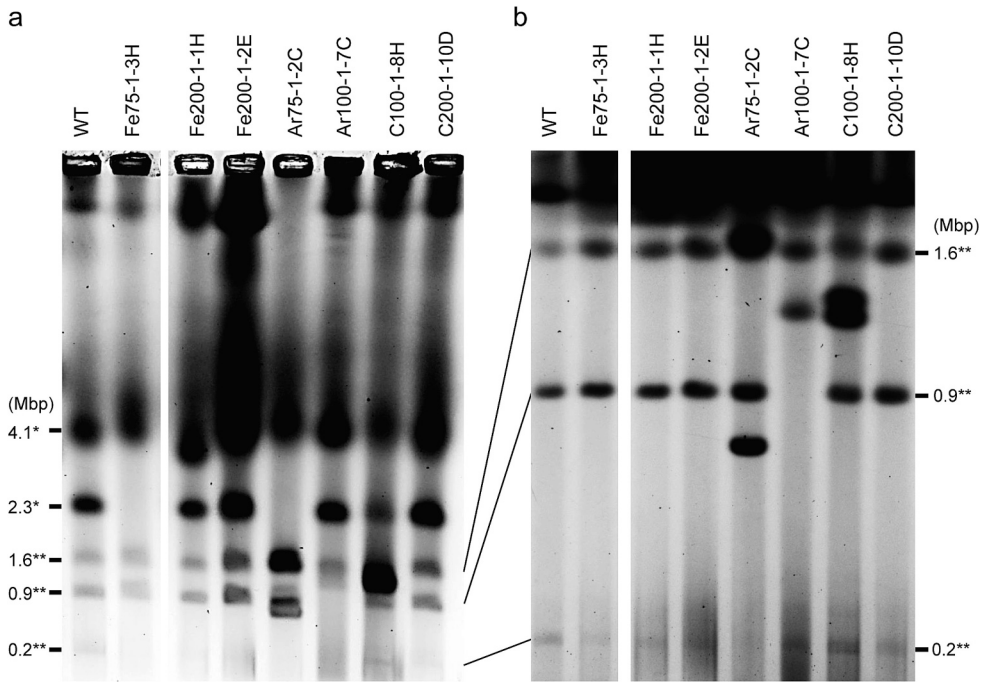

Fig. 7. PFGE patterns of established cell lines after irradiation with heavy-ion beams. (a) Under condition (i) (see Materials and Methods). (b) Under condition (ii). WT denotes the non-irradiated NIES-2152 line.

confirm the location of the centromere, e.g. by searching for centromere-specific repeat sequences.

4.3. *Chromosomal rearrangement induced by heavy-ion beam with higher LET*

The effects of LET on mutagenesis have been reported in *A. thaliana*. Kazama et al. [30] demonstrated that heavy-ion beams with an LET of 290 keV/μm induced large-scale mutations, including indels of >100 bp and chromosomal rearrangements, about 4.4 times more frequently than beams with an LET of 30 keV/μm. This study showed the fragmentation of *P. kessleri* chromosomes after irradiation with heavy-ion beams (Figs. 5 and 6). At the same LET, the number of fragmented chromosomes increased with higher absorbed doses. At the same absorbed dose, a higher LET led to more fragmented chromosomes. Large-scale mutations detected in the whole- genome mutation analysis showed a similar trend (Fig. 8; Supplementary Tables 3 and 4). However, the C100–1-8H line had no significant mutations supporting the chromosome fragmentation detected by PFGE (Fig. 7), indicating the need for further investigation, including obtaining genome sequences at the T2T level, to confirm the effects of LET on *P. kessleri* mutations.

We predicted the functions of genes thought to have lost function in five cell lines in which chromosomal rearrangements were detected (Table 1, Supplementary Table 5). One of the three single-copy genes showed homology to a glutamate/gamma-aminobutyrate antiporter, and mutants of this gene in *Escherichia coli* show a tenfold decrease in resistance to glutamate [67]. The second gene showed homology with the mitochondrial import inner membrane translocase subunit Tim21, which has significant defects in respiratory growth at high temperatures in yeast [68]. The third gene shows homology to a transmembrane GTPase FZO-like gene, and knockout mutants of *FZL* in *A. thaliana* show abnormalities in chloroplast and thylakoid morphology [69]. Mutations in any of these genes may not show phenotypic changes under normal culture conditions, or the mutations may not be visually detectable.

The genome sequence revealed 27 regions with telomeric repeats, more than the number of chromosome ends (20) (Supplementary Fig. 1). In addition, telomeric repeat sequences were found within the scaffold sequence (Scaffolds_1). Many species have telomeric repeat sequences both at the ends of the chromosomes and within the chromosomes [70]. It was hypothesized that some of the telomeric repeat sequences discovered in this study were internal telomeric repeats, and that their translocation to the fragmented chromosome ends may have stabilized the fragmented chromosomes. The Ar75–1-2C line had a large duplicated region adjacent to the translocation with a telomeric repeat sequence (Fig. 8). It is possible that the duplicated region represents a newly formed stable fragmented chromosome.

These results suggest that irradiation with heavy-ion beams can induce chromosomal rearrangements, with some changes being heritable, potentially affecting a range of genes and leading to phenotypic mutants suitable for biomass production.

5. Conclusions

This study revealed that *P. kessleri* has seven A chromosomes and three B chromosomes, as determined by microscopic observation and PFGE analysis. The mean relative fluorescence intensity of the nuclei stained with SYBR Green I at stationary phase was designated as 1C of the nuclear DNA content. During the logarithmic growth phase, the nuclear DNA content fluctuated between 1.1C and 9.7C, while the chromosome number remained constant, indicating that the chromosomes were polytene during multiple cleavage and that endoreduplication occurred in *P. kessleri*.

The use of heavy-ion irradiation led to fragmentation of the chromosomes. The number of fragmented chromosomes increased with higher LET and absorbed doses, but decreased with repeated subcultures. Even after four subcultures, 9.7 % of cells irradiated with 50 Gy iron-ion beam and 3 % of cells irradiated with 75 Gy still had >20 chromosomes, indicating that some fragmented chromosomes were heritable.

The reference genome sequence of *P. kessleri* was refined to 52 scaffolds with an N50 of 2.5 Mbp and a BUSCO value of 98.3 %. Genome-wide mutational analysis of cell lines with stable fragmented chromosomes revealed translocations involving telomeric repeat sequences that may contribute to the stability of fragmented chromosomes. In addition,

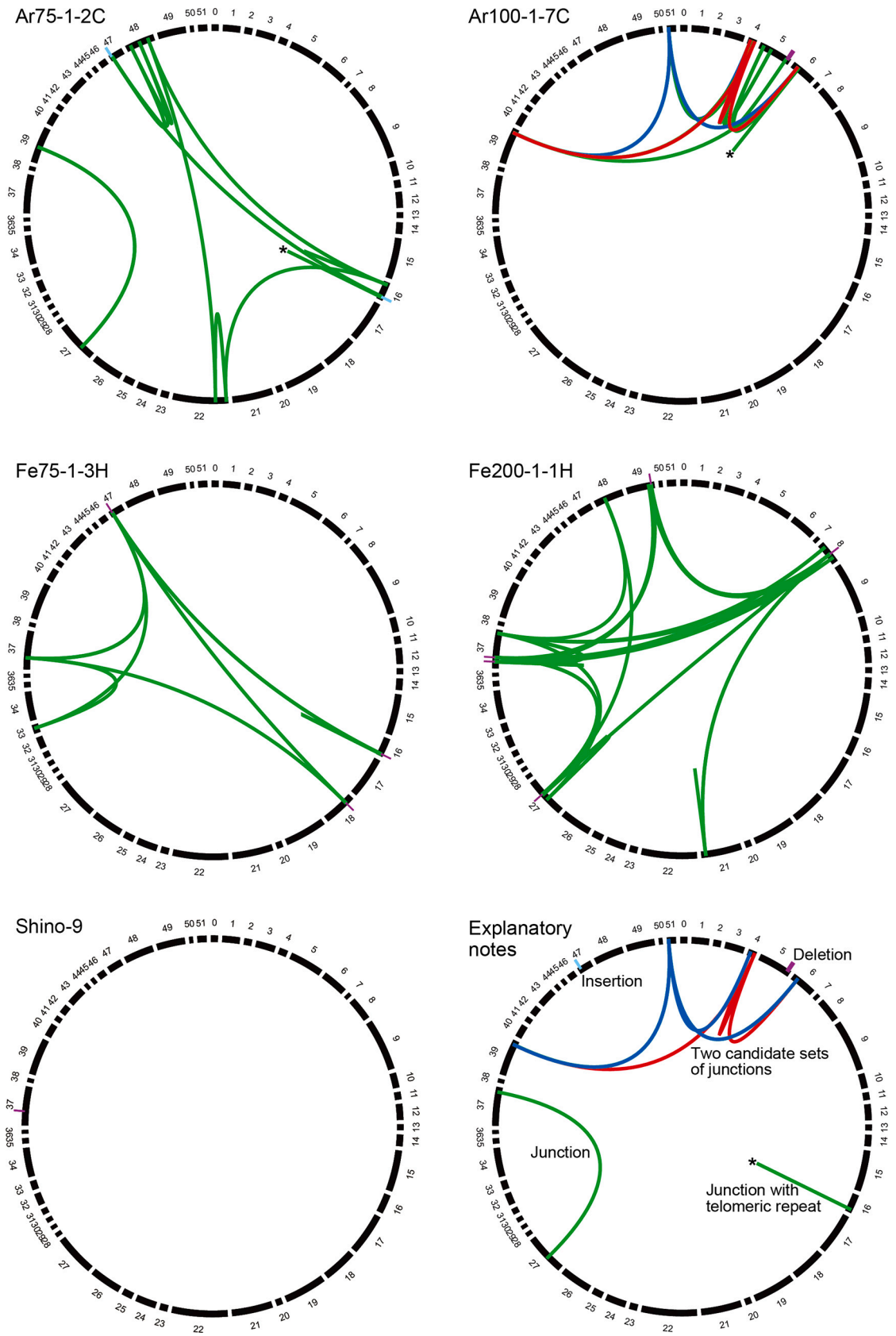

Fig. 8. Circos diagrams illustrating large-scale mutations detected in established cell lines after irradiation with heavy-ion beams. The 52 scaffolds are arranged in a black circle with the corresponding scaffold number marked on the outside. Junctions of large-scale mutations, including large deletions (≥ 100 bp), translocations, and inversions, are plotted as lines inside the circles. The asterisk denotes junctions associated with telomeric repeat regions. The two candidate sets of junctions involving repetitive regions detected in the Ar100–1-7C line could not be identified and are indicated by light blue and red lines, respectively. (For interpretation of the references to colour in this figure legend, the reader is referred to the web version of this article.)

Table 1
Number of breakpoints and mutated genes.

Cell line	Ar-100-1-7C	Ar75–1-2C	Fe200–1-1H	Fe75–1-3H	Shino-9	Total
Breakpoints[a]	33	23	56	20	2	134
Disrupted genes[b]	33	8	14	5	1	61
Genes with predicted functions[c]	17	5	12	3	1	38
Single-copy genes[d]	2	0	1	0	0	3

[a] Total number of breakpoints involved in induced translocations and deletions in each cell line.
[b] Total number of genes disrupted by induced translocations and deletions in each cell line.
[c] Total number of disrupted genes with homology to known genes with predicted functions.
[d] The total number of disrupted genes that are single-copy and have homology to known genes with predicted functions.

the large-scale duplication and deletion were observed, indicating the potential utility of heavy-ion beam irradiation to generate new phenotypic mutants.

CRediT authorship contribution statement

Kotaro Ishii: Writing – original draft, Visualization, Formal analysis, Data curation, Conceptualization. **Madoka Asano:** Visualization, Investigation, Formal analysis. **Yusuke Kazama:** Data curation, Conceptualization. **Tsuyoshi Takeshita:** Visualization, Investigation, Formal analysis. **Kateřina Bišová:** Writing – review & editing. **Vilém Zachleder:** Writing – review & editing. **Atsushi Toyoda:** Investigation, Formal analysis. **Tomoko Abe:** Writing – review & editing. **Shigeyuki Kawano:** Writing – review & editing, Supervision, Resources, Project administration, Funding acquisition, Conceptualization.

Declaration of competing interest

The authors declare that they have no known competing financial interests or personal relationships that could have appeared to influence the work reported in this paper.

Acknowledgements

This work was supported by Program on Open Innovation Platform with Enterprises, Research Institute and Academia, Japan Science and Technology Agency (JST, OPERA, JPMJPO1832) and by JSPS KAKENHI Grant Number JP16H06279 (PAGS) and JP19K06622. We thank the RIKEN Nishina Center and the Center for Nuclear Study, University of Tokyo for the operation of RIBF for performing the ion-beam irradiations, Dr. Atsushi Yoshida (RIKEN) for calculating penetration distances of heavy-ion beams. We are also grateful for allocating computational time of the HOKUSAI BigWaterfall supercomputer at RIKEN ICS.

Appendix A. Supplementary data

Supplementary data to this article can be found online at https://doi.org/10.1016/j.algal.2025.104047.

Data availability

The data presented in this study are openly available in the DDBJ Sequenced Read Archive, under the accession numbers DRR658186-DRR658197.

References

[1] B. Fernandes, J. Teixeira, G. Dragone, A.A. Vicente, S. Kawano, K. Bišová, P. Přibyl, V. Zachleder, M. Vítová, Relationship between starch and lipid accumulation induced by nutrient depletion and replenishment in the microalga *Parachlorella kessleri*, Bioresour. Technol. 144 (2013) 268–274, https://doi.org/10.1016/j.biortech.2013.06.096.
[2] X. Li, P. Přibyl, K. Bišová, S. Kawano, V. Cepák, V. Zachleder, M. Čížková, I. Brányiková, M. Vítová, The microalga *Parachlorella kessleri*—a novel highly efficient lipid producer, Biotechnol. Bioeng. 110 (2013) 97–107, https://doi.org/10.1002/bit.24595.
[3] Y. Mizuno, A. Sato, K. Watanabe, A. Hirata, T. Takeshita, S. Ota, N. Sato, V. Zachleder, M. Tsuzuki, S. Kawano, Sequential accumulation of starch and lipid induced by sulfur deficiency in *Chlorella* and *Parachlorella* species, Bioresour. Technol. 129 (2013) 150–155, https://doi.org/10.1016/j.biortech.2012.11.030.
[4] T. Takeshita, S. Ota, T. Yamazaki, A. Hirata, V. Zachleder, S. Kawano, Starch and lipid accumulation in eight strains of six *Chlorella* species under comparatively high light intensity and aeration culture conditions, Bioresour. Technol. 158 (2014) 127–134, https://doi.org/10.1016/j.biortech.2014.01.135.
[5] K. Bišová, V. Zachleder, Cell-cycle regulation in green algae dividing by multiple fission, J. Exp. Bot. 65 (2014) 2585–2602, https://doi.org/10.1093/jxb/ert466.
[6] M. Vítová, K. Bišová, D. Umysová, M. Hlavová, S. Kawano, V. Zachleder, M. Čížková, *Chlamydomonas reinhardtii*: duration of its cell cycle and phases at growth rates affected by light intensity, Planta 233 (2011) 75–86, https://doi.org/10.1007/s00425-010-1282-y.
[7] V. Zachleder, O. Schläfli, A. Boschetti, Growth-controlled oscillation in activity of histone H1 kinase during the cell cycle of *Chlamydomonas reinhardtii* (Chlorophyta), J. Phycol. 33 (1997) 673–681, https://doi.org/10.1111/j.0022-3646.1997.00673.x.
[8] V. Zachleder, K. Bišová, M. Vítová, The cell cycle of microalgae, M.A. Borowitzka, J. Beardall, J.A. Raven (Eds.), The Physiology of Microalgae, Springer, Dordrecht, 2016, Volume 6, pp. 3–46.
[9] V. Zachleder, I.N. Ivanov, V. Kselíková, V. Bialevich, M. Vítová, S. Ota, T. Takeshita, S. Kawano, K. Bišová, Characterization of growth and cell cycle events affected by light intensity in the green alga *Parachlorella kessleri*: a new model for cell cycle research, Biomolecules 11 (2021) 891, https://doi.org/10.3390/biom11060891.
[10] D.L. Reinecke, A. Castillo-Flores, S. Boussiba, A. Zarka, Polyploid polynuclear consecutive cell-cycle enables large genome-size in *Haematococcus pluvialis*, Algal Res. 33 (2018) 456–461, https://doi.org/10.1016/j.algal.2018.06.013.
[11] H.O. Lee, J.M. Davidson, R.J. Duronio, Endoreplication: polyploidy with purpose, Genes Dev. 23 (2009) 2461–2477, https://doi.org/10.1101/gad.1829209.
[12] J. Joubès, C. Chevalier, Endoreduplication in higher plants, in: D. Inzé (Ed.), The Plant Cell Cycle, Springer, Dordrecht, 2000, pp. 191–201, https://doi.org/10.1007/978-94-010-0936-2.
[13] W. Nagl, DNA endoreduplication and polyteny understood as evolutionary strategies, Nature 261 (1976) 614–615, https://doi.org/10.1038/261614a0.
[14] M. Bourdon, J. Pirrello, C. Cheniclet, O. Coriton, M. Bourge, S. Brown, A. Moïse, M. Peypelut, V. Rouyère, J.P. Renaudin, C. Chevalier, N. Frangne, Evidence for karyoplasmic homeostasis during endoreduplication and a ploidy-dependent increase in gene transcription during tomato fruit growth, Development 139 (2012) 3817–3826, https://doi.org/10.1242/dev.084053.
[15] B. Dzhambazov, D. Belkinova, R. Mladenov, Karyotypic analysis of two algae species *Scenedesmus incrassatulus* Bohl and *Scenedesmus antennatus* Bréb (Chlorophyta, Chlorococcales), Hereditas 139 (2003) 35–40, https://doi.org/10.1111/j.1601-5223.2003.01740.x.
[16] B. Dzhambazov, R. Mladenov, I. Teneva, D. Belkinova, Karyotypic differences and evolutionary tendencies of some species from the subgenus *Obliquodesmus* Mlad. Of genus *Scenedesmus* Meyen (Chlorophyta, Chlorococcales), J. Genet. 85 (2006) 39–44, https://doi.org/10.1007/BF02728968.
[17] J.D. Sánchez-Gárate, L.A. Cira-Chavez, N.P. Rout, Visualization of smaller chromosomes from unicellular microalgae, Rev. Bras. Bot. 43 (2020) 633–641, https://doi.org/10.1007/s40415-020-00619-2.
[18] R. Zidarova, D. Temniskova, B. Dzhambazov, Karyological and endosymbiotic notes on two Choricystis species (Trebouxiophyceae, Chlorophyta), Biologia 64 (2009) 43–47, https://doi.org/10.2478/s11756-009-0009-7.
[19] N. Shikazono, Y. Yokota, S. Kitamura, C. Suzuki, H. Watanabe, S. Tano, A. Tanaka, Mutation rate and novel *tt* mutants of *Arabidopsis thaliana* induced by carbon ions, Genetics 163 (2003) 1449–1455, https://doi.org/10.1093/genetics/163.4.1449.
[20] A. Tanaka, N. Shikazono, Y. Hase, Studies on biological effects of ion beams on lethality, molecular nature of mutation, mutation rate, and spectrum of mutation phenotype for mutation breeding in higher plants, J. Radiat. Res. 51 (2010) 223–233, https://doi.org/10.1269/jrr.09143.
[21] T. Abe, H. Ryuto, N. Fukunishi, Ion beam radiation mutagenesis, Q.Y. Shu, B.P. Forster, H. Nakagawa (Eds.), Plant Mutation Breeding and Biotechnology, CABI, Oxfordshire, 2012, pp. 99–106.
[22] T. Abe, Y. Kazama, T. Hirano, Ion beam breeding and gene discovery for function analyses using mutants, Nucl. Phys. News 25 (2015) 30–34, https://doi.org/10.1080/10619127.2015.1104130.
[23] T. Abe, H. Ichida, Y. Hayashi, R. Morita, Y. Shirakawa, K. Ishii, T. Sato, H. Saito, Y. Okumoto, Ion beam mutagenesis - an innovative and effective method for plant breeding and gene discovery, S. Sivasankar, T.H.N. Ellis, L. Jankuloski, I. Ingelbrecht (Eds.), Mutation breeding, genetic diversity and crop adaptation to climate change, CABI, Oxfordshire, 2021, pp. 411–423.

[24] K. Ishii, S. Kawano, T. Abe, Creation of green innovation and functional gene analyses using heavy-ion beam breeding, Cytologia 86 (2021) 273–274, https://doi.org/10.1508/cytologia.86.273.
[25] L. Ma, F. Kong, K. Sun, T. Wang, T. Guo, From classical radiation to modern radiation: past, present, and future of radiation mutation breeding, Front. Public Health 9 (2021) 768071, https://doi.org/10.3389/fpubh.2021.768071.
[26] Y. Kazama, H. Saito, Y.Y. Yamamoto, Y. Hayashi, H. Ichida, H. Ryuto, N. Fukunishi, T. Abe, LET-dependent effects of heavy-ion beam irradiation in *Arabidopsis thaliana*, Plant Biotechnol. 25 (2008) 113–117, https://doi.org/10.5511/plantbiotechnology.25.113.
[27] T. Hirano, Y. Kazama, S. Ohbu, Y. Shirakawa, Y. Liu, T. Kambara, N. Fukunishi, T. Abe, Molecular nature of mutations induced by high-LET irradiation with argon and carbon ions in *Arabidopsis thaliana*, Mutat. Res. 735 (2012) 19–31, https://doi.org/10.1016/j.mrfmmm.2012.04.010.
[28] S. Ota, T. Matsuda, T. Takeshita, T. Yamazaki, Y. Kazama, T. Abe, S. Kawano, Phenotypic spectrum of *Parachlorella kessleri* (Chlorophyta) mutants produced by heavy-ion irradiation, Bioresour. Technol. 149 (2013) 432–438, https://doi.org/10.1016/j.biortech.2013.09.079.
[29] T. Takeshita, I.N. Ivanov, K. Oshima, K. Ishii, H. Kawamoto, S. Ota, T. Yamazaki, A. Hirata, Y. Kazama, T. Abe, M. Hattori, K. Bišová, V. Zachleder, S. Kawano, Comparison of lipid productivity of *Parachlorella kessleri* heavy-ion beam irradiation mutant PK4 in laboratory and 150-L mass bioreactor, identification and characterization of its genetic variation, Algal Res. 35 (2018) 416–426, https://doi.org/10.1016/j.algal.2018.09.005.
[30] Y. Kazama, K. Ishii, T. Hirano, T. Wakana, M. Yamada, S. Ohbu, T. Abe, Different mutational function of low- and high-linear energy transfer heavy-ion irradiation demonstrated by whole-genome resequencing of Arabidopsis mutants, Plant J. 92 (2017) 1020–1030, https://doi.org/10.1111/tpj.13738.
[31] K. Ishii, Y. Kazama, T. Hirano, J.A. Fawcett, M. Sato, M.Y. Hirai, F. Sakai, Y. Shirakawa, S. Ohbu, T. Abe, Genomic view of heavy-ion-induced deletions associated with distribution of essential genes in *Arabidopsis thaliana*, Front. Plant Sci. 15 (2024) 1352564, https://doi.org/10.3389/fpls.2024.1352564.
[32] S. Ota, K. Oshima, T. Yamazaki, S. Kim, Z. Yu, M. Yoshihara, K. Takeda, T. Takeshita, A. Hirata, K. Bišová, V. Zachleder, M. Hattori, S. Kawano, Highly efficient lipid production in the green alga *Parachlorella kessleri*: draft genome and transcriptome endorsed by whole-cell 3D ultrastructure, Biotechnol. Biofuels 9 (2016) 13, https://doi.org/10.1186/s13068-016-0424-2.
[33] Y. Kasai, S. Takagi, S. Ota, K. Ishii, T. Takeshita, S. Kawano, S. Harayama, Development of a CRISPR/Cas9-mediated gene-editing method to isolate a mutant of the unicellular green alga *Parachlorella kessleri* strain NIES-2152 with improved lipid productivity, Biotechnol. Biofuels 17 (2024) 36, https://doi.org/10.1186/s13068-024-02484-7.
[34] Z.L. Payne, G.M. Penny, T.N. Turner, S.K. Dutcher, A gap-free genome assembly of *Chlamydomonas reinhardtii* and detection of translocations induced by CRISPR-mediated mutagenesis, Plant Commun. 4 (2023) 100493, https://doi.org/10.1016/j.xplc.2022.100493.
[35] M.S. Roth, S.J. Cokus, S.D. Gallaher, A. Walter, D. Lopez, E. Erickson, B. Endelman, D. Westcott, C.A. Larabell, S.S. Merchant, M. Pellegrini, K.K. Niyogi, Chromosome-level genome assembly and transcriptome of the green alga *Chromochloris zofingiensis* illuminates astaxanthin production, Proc. Natl. Acad. Sci. USA 114 (2017) E4296–E4305, https://doi.org/10.1073/pnas.1619928114.
[36] Y. Xu, H. Wang, S.K. Sahu, L. Li, H. Liang, G. Günther, G.K.S. Wong, B. Melkonian, M. Melkonian, H. Liu, S. Wang, Chromosome-level genome of *Pedinomonas minor* (Chlorophyta) unveils adaptations to abiotic stress in a rapidly fluctuating environment, New Phytol. 235 (2022) 1409–1425, https://doi.org/10.1111/nph.18220.
[37] J.H. Wisecaver, R.P. Auber, A.L. Pendleton, N.F. Watervoort, T.R. Fallon, O. L. Riedling, S.R. Manning, B.S. Moore, W.W. Driscoll, Extreme genome diversity and cryptic speciation in a harmful algal-bloom-forming eukaryote, Curr. Biol. 33 (2023) 2246–2259.e8, https://doi.org/10.1016/j.cub.2023.05.003.
[38] D.J. Giguere, A.T. Bahcheli, S.S. Slattery, R.R. Patel, T.S. Browne, M. Flatley, B. J. Karas, D.R. Edgell, G.B. Gloor, Telomere-to-telomere genome assembly of Phaeodactylum tricornutum, PeerJ 5 (2022) e13607, https://doi.org/10.7717/peerj.13607.
[39] K. Ogawa, S. Kawano, T. Kuroiwa, Stabilization and isolation of mitochondrial Nucleifrom *Physarum polycephalum*, Cell Struct. Funct. 5 (1980) 165–174, https://doi.org/10.1247/csf.5.165.
[40] J.S. Kim, N. Davidson, Electron microscope heteroduplex study of sequence relations of T2, T4, and T6 bacteriophage DNAs, Virology 57 (1974) 93–111, https://doi.org/10.1016/0042-6822(74)90111-1.
[41] C.A. Schneider, W.S. Rasband, K.W. Eliceiri, NIH image to ImageJ: 25 years of image analysis, Nat. Methods 9 (2012) 671–675, https://doi.org/10.1038/nmeth.2089.
[42] Y. Kamimura, H. Tanaka, Y. Kobayashi, T. Shikanai, Y. Nishimura, Chloroplast nucleoids as a transformable network revealed by live imaging with a microfluidic device, Commun. Biol. 1 (2018) 47, https://doi.org/10.1038/s42003-018-0055-1.
[43] S. Koren, B.P. Walenz, K. Berlin, J.R. Miller, A.M. Phillippy, Canu: scalable and accurate long-read assembly via adaptive k-mer weighting and repeat separation, Genome Res. 27 (2017) 722–736, https://doi.org/10.1101/gr.215087.116.
[44] B.J. Walker, T. Abeel, T. Shea, M. Priest, A. Abouelliel, S. Sakthikumar, C. A. Cuomo, Q. Zeng, J. Wortman, S.K. Young, A.M. Earl, Pilon: an integrated tool for comprehensive microbial variant detection and genome assembly improvement, PLoS One 9 (2014) e112963, https://doi.org/10.1371/journal.pone.0112963.
[45] M. Qin, S. Wu, A. Li, F. Zhao, H. Feng, L. Ding, J. Ruan, LRScaf: improving draft genomes using long noisy reads, BMC Genomics 20 (2019) 955, https://doi.org/10.1186/s12864-019-6337-2.
[46] C. Camacho, G. Coulouris, V. Avagyan, N. Ma, J. Papadopoulos, K. Bealer, T. L. Madden, BLAST+: architecture and applications, BMC Bioinformatics 10 (2009) 421, https://doi.org/10.1186/1471-2105-10-421.
[47] A. Lomsadze, V. Ter-Hovhannisyan, Y.O. Chernoff, M. Borodovsky, Gene identification in novel eukaryotic genomes by self-training algorithm, Nucleic Acids Res. 33 (2005) 6494–6506, https://doi.org/10.1093/nar/gki937.
[48] M. Manni, M.R. Berkeley, M. Seppey, F.A. Simão, E.M. Zdobnov, BUSCO update: novel and streamlined workflows along with broader and deeper phylogenetic coverage for scoring of eukaryotic, prokaryotic, and viral genomes, Mol. Biol. Evol. 38 (2021) 4647–4654, https://doi.org/10.1093/molbev/msab19.
[49] J. Fulnečková, T. Hasíková, J. Fajkus, A. Lukešová, M. Eliáš, E. Sýkorová, Dynamic evolution of telomeric sequences in the green algal order Chlamydomonadales, Genome Biol. Evol. 4 (2012) 248–264, https://doi.org/10.1093/gbe/evs007.
[50] H. Li, Aligning sequence reads, clone sequences and assembly contigs with BWA-MEM, arXiv:1303.3997v2 [q-bio.GN], doi:10.48550/arXiv.1303.3997.
[51] J.T. Robinson, H. Thorvaldsdottir, W. Winckler, M. Guttman, E.S. Lander, G. Getz, J.P. Mesirov, Integrative genomics viewer, Nat. Biotechnol. 29 (2011) 24–26, https://doi.org/10.1038/nbt.1754.
[52] M. Matsuzaki, O. Misumi, T. Shin-I, S. Maruyama, M. Takahara, S. Miyagishima, T. Mori, K. Nishida, F. Yagisawa, K. Nishida, Y. Yoshida, Y. Nishimura, S. Nakao, T. Kobayashi, Y. Momoyama, T. Higashiyama, A. Minoda, M. Sano, H. Nomoto, K. Oishi, H. Hayashi, F. Ohta, S. Nishizaka, S. Haga, S. Miura, T. Morishita, Y. Kabeya, K. Terasawa, Y. Suzuki, Y. Ishii, S. Asakawa, H. Takano, N. Ohta, H. Kuroiwa, K. Tanaka, N. Shimizu, S. Sugano, N. Sato, H. Nozaki, N. Ogasawara, Y. Kohara, T. Kuroiwa, Genome sequence of the ultrasmall unicellular red alga *Cyanidioschyzon merolae* 10D, Nature 428 (2004) 653–657, https://doi.org/10.1038/nature02398.
[53] K. Ishii, Y. Kazama, T. Hirano, M. Hamada, Y. Ono, M. Yamada, T. Abe, AMAP: a pipeline for whole-genome mutation detection in *Arabidopsis thaliana*, Genes Genet. Syst. 91 (2016) 229–233, https://doi.org/10.1266/ggs.15-00078.
[54] Feldman and Levy, Wheat Evolution and Domestication, Springer, Cham, 2023.
[55] B. John B, Population Cytogenetics, Edward Arnold, London, 1976.
[56] M.M. Swim, K.E. Kaeding, P.M. Ferree, Impact of a selfish B chromosome on chromatin dynamics and nuclear organization in *Nasonia*, J. Cell Sci. 125 (2012) 5241–5249, https://doi.org/10.1242/jcs.113423.
[57] R.N. Jones, Tansley review no 85 - B chromosomes in plants, New Phytol. 131 (1995) 411–434, https://doi.org/10.1111/j.1469-8137.1995.tb03079.x.
[58] R.N. Jones, W. Viegas, A. Houben, A century of B chromosomes in plants: so what? Ann. Bot. 101 (2008) 767–775, https://doi.org/10.1093/aob/mcm167.
[59] G. Blanc, G. Duncan, I. Agarkova, M. Borodovsky, J. Gurnon, A. Kuo, E. Lindquist, S. Lucas, J. Pangilinan, J. Polle, A. Salamov, A. Terry, T. Yamada, D.D. Dunigan, I. V. Grigoriev, J.M. Claverie, J.L. Van Etten, The *Chlorella variabilis* NC64A genome reveals adaptation to photosymbiosis, coevolution with viruses, and cryptic sex, Plant Cell 22 (2010) 2943–2955, https://doi.org/10.1105/tpc.110.076406.
[60] T. Higashiyama, T. Yamada, Electrophoretic karyotyping and chromosomal gene mapping of *Chlorella*, Nucleic Acids Res. 19 (1991) 6191–6195, https://doi.org/10.1093/nar/19.22.6191.
[61] G. Blanc, I. Agarkova, J. Grimwood, A. Kuo, A. Brueggeman, D.D. Dunigan, J. Gurnon, I. Ladunga, E. Lindquist, S. Lucas, J. Pangilinan, T. Pröschold, A. Salamov, J. Schmutz, D. Weeks, T. Yamada, A. Lomsadze, M. Borodovsky, J. M. Claverie, I.V. Grigoriev, J.L. Van Etten, The genome of the polar eukaryotic microalga *Coccomyxa subellipsoidea* reveals traits of cold adaptation, Genome Biol. 13 (2012) R39, https://doi.org/10.1186/gb-2012-13-5-r39.
[62] S. Arai, H. Takahashi, H. Takano, A. Sakai, S. Kawano, Isolation, characterization, and chromosome mapping of an actin gene from the primitive green alga, *Nannochloris bacillaris* (Chorophyceae), J. Phycol. 34 (1998) 477–485, https://doi.org/10.1046/j.1529-8817.1998.340477.x.
[63] H. Nozaki, H. Takano, O. Misumi, K. Terasawa, M. Matsuzaki, S. Maruyama, K. Nishida, F. Yagisawa, Y. Yoshida, T. Fujiwara, S. Takio, K. Tamura, S.J. Chung, S. Nakamura, H. Kuroiwa, K. Tanaka, N. Sato, T. Kuroiwa, A 100%-complete sequence reveals unusually simple genomic features in the hot-spring red alga *Cyanidioschyzon merolae*, BMC Biol. 5 (2007) 28, https://doi.org/10.1186/1741-7007-5-28.
[64] A.Z. Worden, J.H. Lee, T. Mock, P. Rouzé, M.P. Simmons, A.L. Aerts, A.E. Allen, M. L. Cuvelier, E. Derelle, M.V. Everett, E. Foulon, J. Grimwood, H. Gundlach, B. Henrissat, C. Napoli, S.M. McDonald, M.S. Parker, S. Rombauts, A. Salamov, P. Von Dassow, J.H. Badger, P.M. Coutinho, E. Demir, I. Dubchak, C. Gentemann, W. Eikrem, J.E. Gready, U. John, W. Lanier, E.A. Lindquist, S. Lucas, K.F.X. Mayer, H. Moreau, F. Not, R. Otillar, O. Panaud, J. Pangilinan, I. Paulsen, B. Piegu, A. Poliakov, S. Robbens, J. Schmutz, E. Toulza, T. Wyss, A. Zelensky, K. Zhou, E. V. Armbrust, D. Bhattacharya, U.W. Goodenough, Y. Van de Peer, I.V. Grigoriev, Green evolution and dynamic adaptations revealed by genomes of the marine picoeukaryotes *Micromonas*, Science 324 (2009) 268–272, https://doi.org/10.1126/science.1167222.
[65] B. Palenik, J. Grimwood, A. Aerts, P. Rouzé, A. Salamov, N. Putnam, C. Dupont, R. Jorgensen, E. Derelle, S. Rombauts, K. Zhou, R. Otillar, S.S. Merchant, S. Podell, T. Gaasterland, C. Napoli, K. Gendler, A. Manuell, V. Tai, O. Vallon, G. Piganeau, S. Jancek, M. Heijde, K. Jabbari, C. Bowler, M. Lohr, S. Robbens, G. Werner, I. Dubchak, G.J. Pazour, Q. Ren, I. Paulsen, C. Delwiche, J. Schmutz, D. Rokhsar, Y. Van de Peer, H. Moreau, I.V. Grigoriev, The tiny eukaryote *Ostreococcus* provides genomic insights into the paradox of plankton speciation, Proc. Natl. Acad. Sci. USA 104 (2007) 7705–7710, https://doi.org/10.1073/pnas.0611046104.
[66] C.L.C. Goemann, R. Wilkinson, W. Henriques, H. Bui, H.M. Goemann, R.P. Carlson, S. Viamajala, R. Gerlach, B. Wiedenheft, Genome sequence, phylogenetic analysis, and structure-based annotation reveal metabolic of *Chlorella* SLA-04, Algal Res. 69 (2023) 102943, https://doi.org/10.1016/j.algal.2022.102943.

[67] B.M. Hersh, F.T. Farooq, D.N. Barstad, D.L. Blankenhorn, J.L. Slonczewski, A glutamate-dependent acid resistance gene in *Escherichia coli*, J. Bacteriol. 178 (1996) 3978–3981, https://doi.org/10.1128/jb.178.13.3978-3981.1996.
[68] M. van der Laan, N. Wiedemann, D.U. Mick, B. Guiard, P. Rehling, N. Pfanner, A role for Tim21 in membrane-potential-dependent preprotein sorting in mitochondria, Curr. Biol. 16 (2006) 2271–2276, https://doi.org/10.1016/j.cub.2006.10.025.
[69] M. Landoni, A. De Francesco, S. Bellatti, M. Delledonne, A. Ferrarini, L. Venturini, R. Pilu, M. Bononi, C. Tonelli, A mutation in the *FZL* gene of *Arabidopsis* causing alteration in chloroplast morphology results in a lesion mimic phenotype, J. Exp. Bot. 64 (2013) 4313–4328, https://doi.org/10.1093/jxb/ert237.
[70] J. Fulnečková, T. Ševčíková, J. Fajkus, A. Lukešová, M. Lukeš, Č. Vlček, B.F. Lang, E. Kim, M. Eliáš, E. Sýkorová, A broad phylogenetic survey unveils the diversity and evolution of telomeres in eukaryotes, Genome Biol. Evol. 5 (2013) 468–7483, https://doi.org/10.1093/gbe/evt019.

Update

Algal Research

Volume 90, Issue , August 2025, Page

DOI: https://doi.org/10.1016/j.algal.2025.104108

Algal Research 90 (2025) 104108

Contents lists available at ScienceDirect

Algal Research

journal homepage: www.elsevier.com/locate/algal

Corrigendum

Corrigendum to "Internal ploidy and heritable chromosome fragmentation in *Parachlorella kessleri*" [Algal. Res. 89 (2025) 104047]

Kotaro Ishii [a,b,1], Madoka Asano [c,1], Yusuke Kazama [a,d], Tsuyoshi Takeshita [e], Kateřina Bišová [f], Vilém Zachleder [f,2], Atsushi Toyoda [g], Tomoko Abe [a], Shigeyuki Kawano [c,e,*]

[a] *RIKEN Nishina Center for Accelerator-Based Science, 2-1 Hirosawa, Wako, Saitama 351-0198, Japan*
[b] *Department of Radiation Measurement and Dose Assessment, Institute for Radiological Science, National Institutes for Quantum Science and Technology, 4-9-1 Anagawa, Inage-ku, Chiba 263-8555, Japan*
[c] *Department of Integrated Biosciences, Graduate School of Frontier Sciences, The University of Tokyo, 5-1-5 Kashiwa-no-ha, Kashiwa, Chiba 277-8561, Japan*
[d] *Department of Bioscience and Biotechnology, Fukui Prefectural University, 4-1-1 Kenjojima, Matsuoka, Eiheiji-cho, Yoshida-gun, Fukui 910-1195, Japan*
[e] *Functional Biotechnology Project, Life Science Data Research Center, Graduate School of Frontier Sciences, 503 Kashiwanoha Campus Station Satellite, The University of Tokyo, 178-4-4 Wakashiba, Kashiwa, Chiba 277-0871, Japan*
[f] *Laboratory of Cell Cycles of Algae, Centre Algatech, Institute of Microbiology of the Czech Academy of Sciences, 37981 Třeboň, Czech Republic*
[g] *Department of Genomics and Evolutionary Biology, National Institute of Genetics, 1111 Yata, Mishima, Shizuoka 411-8540, Japan*

The authors regret that the Data availability section was incomplete. Accordingly, a corrigendum for Data availability is provided.

Data availability

The data presented in this study are openly available in the DDBJ Sequence Read Archive under the accession numbers BAAHLN010000001–BAAHLN010000052, DRR658186–DRR658197, and DRR659504.

The authors would like to apologise for any inconvenience caused.

DOI of original article: https://doi.org/10.1016/j.algal.2025.104047.

* Corresponding author at: Functional Biotechnology Project, Life Science Data Research Center, Graduate School of Frontier Sciences, 503 Kashiwanoha Campus Station Satellite, The University of Tokyo, 178-4-4 Wakashiba, Kashiwa, Chiba 277-8561, Japan.
E-mail address: kawano@edu.k.u-tokyo.ac.jp (S. Kawano).
[1] These authors equally contributed to this work.
[2] Deceased.

https://doi.org/10.1016/j.algal.2025.104108

Available online 27 May 2025